Surface deformation of Ar+ ion collision process via molecular dynamics simulation with comparison to experiment

Shin-ichi Satake,[1,a)] Sadao Momota,[2] Shun Yamashina,[1] Masahiko Shibahara,[3] and Jun Taniguchi[1]

[1]*Department of Applied Electronics, Tokyo University of Science, 2641 Yamazaki, Noda, Chiba 278-8510, Japan*
[2]*Department of Intelligent Mechanical Systems Engineering, Kochi University of Technology, 185 Miyanokuchi, Tosayamada, Kami, Kochi 782-8502, Japan*
[3]*Department of Mechanical Engineering, Osaka University, 2-1 Yamada-oka, Suita, Osaka 565-0871, Japan*

Molecular dynamics simulations of Ar ion collision on a Si surface using an optimized potential function were carried out in the case of the acceleration voltages of 50 keV for Ar ions. A hillock structure was formed by the Ar ion impact on the Si surface. The height of the structure calculated by the simulations corresponded to those of the experiments. The height of the structure was found to be proportional to the fluence of Ar ions. The amorphous structural region was expanded by the progress of the interface region between the amorphous structure and the crystalline structure with increasing the fluence in the depth direction. © *2009 American Institute of Physics.*
[DOI: 10.1063/1.3204640]

I. INTRODUCTION

Focused ion beams (FIBs) are very useful tools in the processes of lithography, doping, deposition, and etching. In particular, the FIB etching and deposition techniques have been widely used for the mask repair and transmission electron microscope (TEM) sample preparation. Recently, these techniques have been extended to the fabrication of three-dimensional (3D) nanostructures. The FIB chemical vapor deposition is used to fabricate 3D nanostructures and the aerial wiring applied to photonic crystals and nanoscale tweezers. The FIB etching, however, has had very limited use in the fabrication and formation of 3D structures, such as predetermined curved shapes, microlens components, and diffractive optical elements, because of the very limited specifications for etching tasks.

Schmuki *et al.*[1] carried out the ion implantation in GaAs with Si^{++} doses ranging from 3×10^{13} to 3×10^{16} cm^{-2} using a FIB. They found that the protrusions of the ion beam treated areas are in the range of 1–15 nm in heights and an increase in surface roughness. Recently, a surface deformation at the nanometer precision on a Si surface was systematically achieved in experiments with a Ga ion beam collision process after an etch pit process created on the Si surface.[2] The height of the deformation was proportional to the ion beam fluence. These experiments demonstrate the requirement for a high-accuracy process technology for the masking at the nanometer precision. On the other hand, a molecular dynamics (MD) simulation can track such phenomena because it can track each ion and atom dynamically. Thus, the MD simulation is a powerful and effective tool for analyzing material deformation by ion beam processing. Humbird *et al.*[3] presented MD simulations of energetic Ar+

ions (20–200 eV) interacting with initially crystalline silicon, with quantitative comparison to experiment. Similar simulations with ions bombardment to Si were also performed by Thijsse *et al.*[4] and Rosso *et al.*[5]

The present study considers nano-order deformation of a surface when the fluence of the irradiation parameter for the calculations is set to be a realistic value for an FIB. Estimations of the deformation height from the simulation results will be important information for the crafting of nanomasks by ion beam processing. Large-scale MD simulations were performed for acceleration voltages of 50 keV for Ar ions. The deformation on the surface caused was analyzed after the ions collided on the Si surface. Moreover, the height of deformation was compared with the experimental value under the same irradiation conditions.

II. COMPUTATIONAL METHOD AND THE MODEL SYSTEMS

We used our previous MD code[6] to investigate the mechanism of surface deformation by Ar ion impacts. In the present MD calculations, the Verlet's algorithm was used for the time integration.

A. Potential function for Si crystal

For the simulation with a Si target, the Tersoff potential function[7] was employed,

$$\phi = \frac{1}{2} \sum_i \sum_{j \neq i} f_c(r_{ij}) \{ f_R(r_{ij}) + b_{ij} f_A(r_{ij}) \}, \tag{1}$$

$$f_R(r) = A \exp(-\lambda r),$$
$$f_A(r) = -B \exp(-\mu r),$$

a)Author to whom correspondence should be addressed. Tel.: +81-4-7124-1501; FAX: +81-4-7122-9195. Electronic mail: satake@te.noda.tus.ac.jp.

TABLE I. Tersoff potential parameters for Si.

	Si
A (eV)	1.8308×10^3
B (eV)	4.7118×10^2
λ (Å^{-1})	2.4799
μ (Å^{-1})	1.7322
n	7.8734×10^{-1}
β	1.1000×10^{-6}
c	1.0039×10^5
d	1.6217×10^1
h	-5.9825×10^{-1}
R (Å)	2.7
S (Å)	3

FIG. 1. Computational domain.

$$f_c(r) = \begin{cases} 1, & r < R \\ \dfrac{1}{2} + \dfrac{1}{2}\cos\dfrac{\pi(r-R)}{S-R}, & R < r < S \\ 0 & r > S, \end{cases} \quad (2)$$

$$b_{ij} = (1 + \beta^n \zeta_{ij}^n)^{-1/2n}, \quad \zeta_{ij} = \sum_{k \neq i,j} f_c(r_{ik}) g(\theta_{ijk}),$$

$$g(\theta) = 1 + \frac{c^2}{d^2} - \frac{c^2}{d^2 + (h - \cos\theta)^2}. \quad (3)$$

Here i, j, and k label the atoms of the system, r_{ij} is the length of the ij bond, and θ_{ijk} is the bond angle between bounds ij and jk. The parameters in Eq. (1) are summarized in Table I.

B. Ar ion for Ziegler, Biersack, and Littmark potential

The Ar ion potential is represented by the Ziegler-Biersack-Littmark potential,[8]

$$\phi(r) = \frac{Z_1 Z_2 e^2}{4\pi\varepsilon r_{ij}} \Phi(r),$$

$$\Phi(r) = \sum_{k=1}^{4} c_k \exp\left(-d_k \frac{r_{ij}}{a_u}\right), \quad a_u = \frac{0.8854 a_0}{Z_i^{0.23} + Z_j^{0.23}},$$

$$a_0 = 0.529 \text{ Å}. \quad (4)$$

Here Z_1 and Z_2 are atomic numbers. The detailed parameters are shown in Table II.

C. Computational parameters

The computational domain for the large-scale calculation is shown in Fig. 1. The target domain is 10.7×10.7

TABLE II. Parameters for ZBL potential.

	c_i	d_i
1	0.028 171	0.201 62
2	0.280 22	0.402 9
3	0.509 86	0.942 99
4	0.181 75	3.199 8
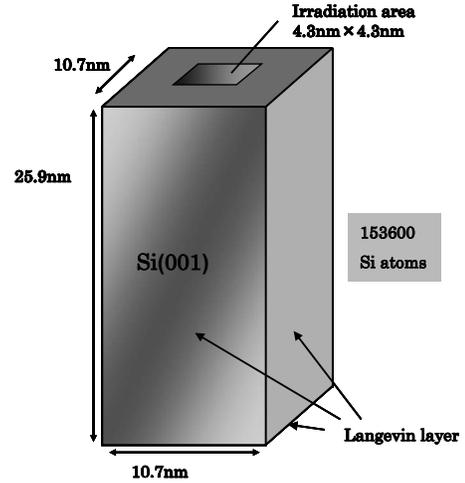
$\times 25.9$ nm^3, consisting of 153 600 Si atoms. Langevin layers as heating bath boundary conditions in the target material were applied except the surface area. The Langevin layers[9] consist of a fixed layer and a temperature control layer. The target surface boundary was represented by a free boundary condition. The initially surface was (001) crystalline at 300 K. The irradiation area is defined as 4.3×4.3 nm^2. At the beginning of each Ar ions impact, the Ar ion was introduced at a random location above the irradiation area on the Si surface. The Ar ion directly impacts to the Si surface without incident angle to the normal direction. The time increment is set to be 0.013 47 fs to track the ion trajectory. The MD simulation under the regular interval impact condition was performed for the acceleration voltage of 50 keV for Ar ion. The interval time between ion impacts is defined as 120 fs, that is, sufficient to simulate the cooling process of the target.

III. DESCRIPTION OF THE EXPERIMENT

In the present study, the irradiation of ion beam was performed by using the irradiation equipment installed at Kochi University of Technology.[10] This equipment is constructed from three parts as shown in Fig. 2. At the production part of ion beam, Ar^{1+} ions were produced by using a 10 GHz NANOGAN (Ref. 11) and accelerated up to 50 keV. At the analysis part of ion beam, the Ar^{1+} ion beam was
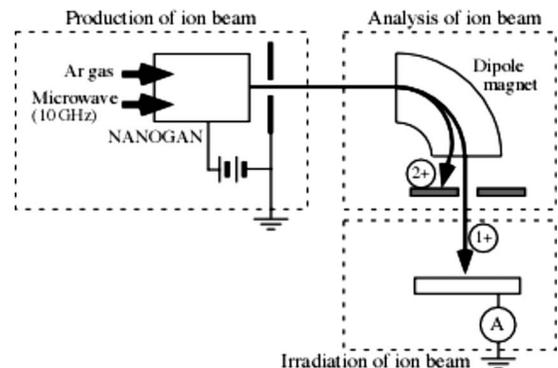
FIG. 2. Schematic picture of the irradiation equipment for Ar^{1+} ion beam.
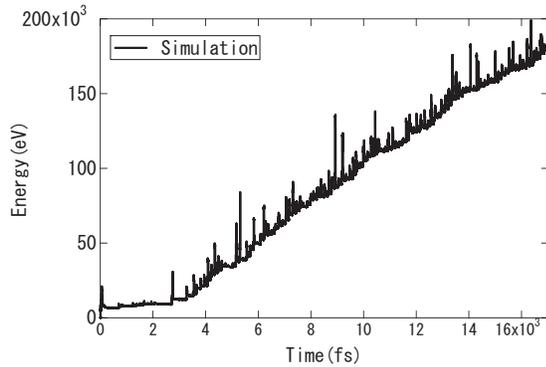
FIG. 3. Time history of the system energy.

FIG. 5. Effects of fluence on local order parameter.

identified and separated by using a dipole magnet. At the irradiation part of ion beam, the separated ion beam was focused and irradiated onto a Si crystal through a Cu stencil mask at room temperature. The thickness of the Si crystal was 525 μm and an oxidized layer on the Si surface was removed by an etching process before the ion irradiation. The Cu stencil mask, whose thickness was 10 μm, has square holes with 7.5 μm sides. The fluence of Ar ions was varied over the range of $3 \times 10^{13} \sim 1 \times 10^{15}$ ion/cm^2. The Si surface was observed by using the SPM-9600 atomic force microscope developed by Shimadzu Corporation.

IV. RESULTS AND DISCUSSION

Figure 3 shows the energy of Si target versus time. The energy enhancement shows moderate profile less than 3000 fs. The energy distribution does not have the peak every 120 fs at this stage and the event of collision cannot be caused every time by the channeling when Ar ion impacts Si atoms. Especially, the channeling occurred at initial state in a high rate statistically, and then the Ar energy cannot be transferred to the upper part of Si substrate. However, when the amorphous region progressed more and more as time advanced, the event of collisions occurred frequently with increase in the amorphous regions. As the results, the system energy suddenly increased at $t=3000$ fs and it is proportional to the time. Figure 4 shows height against fluence amount. The height of the hillock structure provided from MD simulation is defined to be the highest position in the deformed region beyond the initial surface coordinate, and the region is

FIG. 4. Effects of fluence on height of hillock structure.

detected by the tracking distance between Si atoms being less than 3.35 Å. Moreover, the height is expressed as the distance from the initial coordinate before the collision. The height of the hillock structure provided from the experiment is also shown in Fig. 4 as the squire closed symbol, showing the height irradiated by Ar ions when the acceleration energy is 50 keV for the fluences of 3×10^{13}, 1×10^{14}, 3×10^{14}, and 1×10^{15} ion/cm^2. The error bars in the figure show the standard deviation of the observed height of the hillock structure. In MD simulation, when the fluence amount is larger than 4.0×10^{14} ion/cm^2, the height ranged from 1 to 4 nm. The height of the resultant hillock structure is exhibiting an increasing height with increasing fluence amount. Although the beginning of the time for the growth of the height is different for the simulation and the experiment, the height of the hillock structure in the simulation corresponds to the same order as the experimental value, the height of the hillock structure of MD simulation gives lower than that of the experimental results.

To examine the state in the Si target, the local parameter[3] is investigated for the fluence value,

$$\xi = \tfrac{1}{3}(\lambda_x + \lambda_y + \lambda_z), \tag{5}$$

with

$$\lambda_x = \frac{1}{N_{atom}} \sum_{i}^{N} \cos\left(\frac{8\pi}{a} x_i\right), \tag{6}$$

where x_i is the x position of atom i in the lattice and a is the lattice constant. Note that the order parameter switches smoothly from 1 to 0 and shows zero for liquid or amorphous solid and unity for a perfectly crystalline. In Fig. 5 the local value becomes less than unity with the irradiation progressing, that is, the amorphous region is progressed with increasing of the fluence. The amorphous region is developed from the surface; the surface location is larger than the initial coordinate from the bottom boundary (270 Å). Therefore, the surface deformation is caused by the expanding of amorphous region. The time development at the surface region is investigated by visualizing for fluence amounts of 2.99×10^{14}, 4.02×10^{14}, and 6.52×10^{14} ion/cm^2, shown in Fig. 6.

In Fig. 6(a), the concavity is very small. At Fig. 6(b) for 4.2×10^{14} ion/cm^2, after a hillock structure is formed, in the upper region at the surface a few sputtered atoms were observed. Figure 6(c) shows the enhanced deformation. The atoms in each layer move upward. The highest layer at the
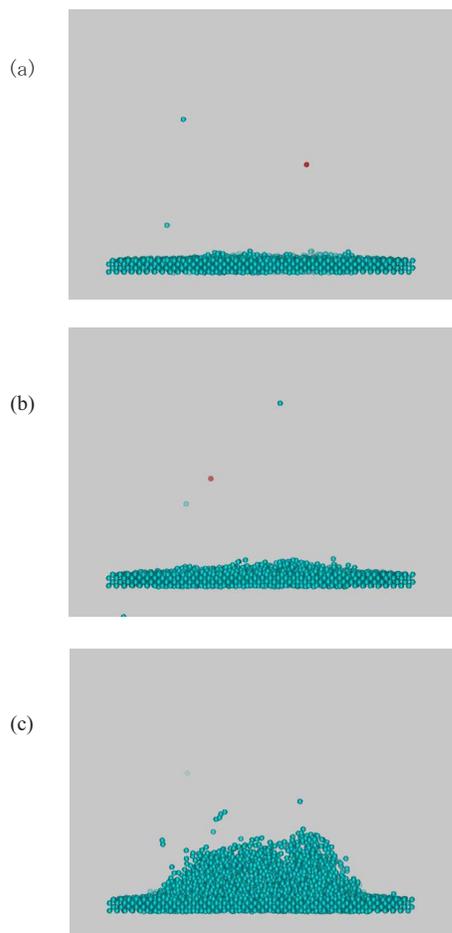
FIG. 6. (Color online) Snapshots at the surface region; (a) 2.99×10^{14} ion/cm^2, (b) 4.02×10^{14} ion/cm^2, and (c) 6.52×10^{14} ion/cm^2.

initial target height is the most greatly enhanced in other figures; the structure is not complete crystalline.

V. CONCLUSIONS

Large-scale MD simulations were carried out to understand the influence of fluence value and surface deformation during ion collisions. A hillock structure was observed and the height of the structure was analyzed and compared to the experimental results. The height of the hillock structure calculated by the MD simulations is in the same order as the experimental value. The height of the hillock structure is 3.77 nm when the fluence value is 6.58×10^{14} ion/cm^2. The growth of the height of the hillock structure is proportional to the fluence amounts. Moreover, the amorphous region is progressed to be proportional to the fluence amount. These phenomena are also observed in the 3D visualization. The deformation at the surface is made of the amorphous structure and the region of the height growth are coincident with the progress of the amorphous region.

[1] P. Schmuki, L. E. Erickson, G. Champion, B. F. Mason, J. Fraser, and C. Moessner, Appl. Phys. Lett. **70**, 1305 (1997).
[2] N. Kawasegi, N. Morita, S. Yamada, N. Takano, T. Oyama, K. Ashida, J. Taniguchi, and I. Miyamoto, (in Japanese),Trans. Jpn. Soc. Mech. Eng., Ser. C **71**, 1754 (2005).
[3] D. B. Humbird, A. Graves, A. E. Stevens, and W. M. M. Kessels, J. Vac. Sci. Technol. A **25**, 1529 (2007).
[4] B. J. Thijsse, T. P. C. Klaver, and E. F. C. Haddeman, Appl. Surf. Sci. **231–232**, 29 (2004).
[5] M. F. Russo, M. Maazouz, L. A. Giannuzzi, C. Chandler, M. Utlaut, and B. J. Garrison, Microsc. Microanal. **14**, 315 (2008).
[6] S. Satake, N. Inoue, J. Taniguchi, and M. Shibahara, J. Phys.: Conf. Ser. **106**, 012013 (2008).
[7] J. Tersoff, Phys. Rev. B **39**, 5566 (1989).
[8] J. F. Ziegler, J. P. Biersack, and U. Littmark, *The Stopping and Range of Ions in Matter* (Pergamon, New York, 1985).
[9] T. Aoki and J. Matsuo, Nucl. Instrum. Methods Phys. Res. B **261**, 639 (2007).
[10] S. Momota, Y. Nojiri, M. Saihara, A. Sakamoto, H. Hamagawa, and K. Hamaguchi, Rev. Sci. Instrum. **75**, 1497 (2004).
[11] C. Bieth, J. L. Bouly, J. C. Curdy, S. Kantas, P. Sortais, P. Sole, and J. L. Vieux-Rochaz, Proceedings of the 14th International Workshop on ECR Sources, Geneva, 1999 (unpublished), p. 147.